World Pendulum – a distributed Remotely Controlled Laboratory (RCL) to measure the earth's gravitational acceleration depending on geographical latitude

S Gröber, M Vetter, B Eckert and H-J Jodl

Department of Physics, University of Technology Kaiserslautern
Erwin-Schrödinger-Straße, D-67663 Kaiserslautern, Germany

Email: groeber@physik.uni-kl.de

Abstract
We suggest to position different string pendulums at different locations on earth and measure at each place the gravitational acceleration (accuracy $\Delta g \sim 0.01$ m/s^2). Each pendulum can be remotely controlled via Internet by a computer located somewhere on earth. The theoretical part describes the physical origin of this phenomenon $g(\varphi)$, that the earth's effective gravitational acceleration g depends on the angle of latitude φ. Then, we present all necessary formula to deduce $g(\varphi)$ from oscillations of a string pendulum. The technical part explains tips and tricks to realize such an apparatus to measure all necessary values with sufficient accuracy. In addition, we justify the precise dimensions of a physical pendulum such that the formula for a mathematical pendulum are applicable to determine $g(\varphi)$ without introducing errors. To conclude, we describe the Internet version – the string pendulum as a Remotely Controlled Laboratory. The teaching relevance and educational value will be discussed in detail at the end of this article such as global experimenting, using Internet and communication techniques in teaching and new ways of teaching and learning methods.

1. Introduction

In the year 1671 the French astronomer Jean Richer (1630 – 1696) travelled from Paris to Cayenne in French-Guyana at the east coast of South America. Together with his colleague Jean Picard who stayed in Paris they wanted to determine the distance between sun and earth by means of a parallax determination taking advantage of the forth coming Mars opposition. But the more famous outcome of these measurements was the fact that Jean Richer discovered that the transported pendulum clock to show a shift of about 2 min/day when he reached Cayenne [1].

Today we know by sure that this observation is caused by the dependency of the gravitational acceleration g from the angle of latitude φ. The gravitational acceleration in Cayenne is $g_{Ca}(4.9°) \sim 9.781$ m/s^2, the one in Paris is $g_{Pa}(48.8°) \sim 9.811$ m/s^2. The smaller acceleration in Cayenne produced a larger oscillation period due to a smaller restoring force at constant mass of the pendulum clock – compared to the situation in Paris. The oscillation period of a mathematical pendulum is

$$T = 2\pi\sqrt{\frac{l}{g}} \tag{1}$$

which gives for the ratio Cayenne/Paris

$$\frac{T_{Ca}}{T_{Pa}} = \sqrt{\frac{g_{Pa}}{g_{Ca}}} = 1.00133\,. \tag{2}$$

The consequence is a shift of 115 s/day ~ 2 min/day confirming Richer's observation.

Here we arrive at the most important and most interesting questions. What are the origins of the dependency $g(\varphi)$? How can one measure this dependency by a string pendulum with sufficient accuracy and by standard equipment available at schools? On top how can we measure $g(\varphi)$ without travelling and moving the experimental set up? In the following we will

- describe our experience in planning and setting up a suitable string pendulum and present the tricks to measure all relevant data,
- explain why it is not an easy task to get appropriate values for g in the framework of an ideal mathematical pendulum,
- present how one can measure at home the gravitational acceleration $g(\varphi)$ without travelling like Richer did, in fact, with an experimental set up that is located quasi at any arbitrary point on earth,
- explain how this experiment can be used at school and at university level,
- open a new way of method of teaching,
- try to exploit modern communication techniques and Internet in the educational system.

2. Origin and mathematical models for $g(\varphi)$

The simplest geophysical model to explain the origin of gravitational acceleration g itself is the earth as a non-rotating, spherical and homogeneous sphere of mass m_e. If one choose as earth's radius R_e the equatorial radius R_{eq}, we end up with a constant acceleration

$$g_0 = \gamma \frac{m_e}{{R_{eq}}^2} = 9{,}798\ \frac{\mathrm{m}}{\mathrm{s}^2}, \tag{3}$$

which is not depending on the degree of latitude (g_0 in figure 1 and 2).

Fig. 1

Fig. 2

In a more refined model, in which the earth is rotating ($\omega = 7.292115 \cdot 10^{-5}$ rad/s), all bodies on the surface of earth are moving on circular paths (figure 1). If we consider now the forces in this rotating coordinate system, we register in point P besides the gravitational acceleration g_0 an additional axially acting centrifugal acceleration, which depends on latitude described by

$$g_c = \omega^2 r = \omega^2 R_e \cos\varphi\ . \tag{4}$$

Its radial component

$$g_{cr} = g_c \cos\varphi \tag{5}$$

reduces the gravitational acceleration g_0 giving an effective acceleration:

$$g_{eff}(\varphi) = g_0 - g_{cr} = \frac{\gamma m_e}{{R_e}^2} - \omega^2 R_e \cos^2\varphi \tag{6}$$

As a consequence, with the assumption $R_e = R_{eq}$ the strength of gravitational acceleration between equator and poles is varying by $\omega^2 R_{eq} = 0.034$ m/s^2 (g_{eff} in figure 2).

In reality the difference in g between the equator and the poles is larger due to the flattening of the earth. The equatorial radius R_{eq} = 6378.137 km is slightly (~ 0.34 %) larger than the polar radius R_p = 6356.752 km. Therefore, we have to refine this model by an ellipsoid, which takes into account the static contribution ($\omega = 0$). In this most recent model (WGS 84 – World Geodetic System [2]) the earth's mass is not considered as to be simply concentrated in one centre. The non-spherical mass distribution causes, for example, an additional gravitational attraction in the case of a mass near equator. This fact and the anisotropic density distribution then has to be calculated by means of proper integrals over the volume of the earth and leads to the formula of normal gravitational acceleration:

$$g_n(\varphi) = 9.780326772 \cdot [1 + 0.00530233 \cdot \sin^2\varphi - 0.00000589 \cdot \sin^2(2\varphi)]\ , \tag{7}$$

where φ in this equation is measured in units of 2π (rad). As a result of this refinement the acceleration g is increasing if going from the equator to the poles by 0.052 m/s^2 or by 0.5 % (g_n in figure 2). In fact, the increase of g_n near equator ($|\varphi| \sim 0° - 30°$) and near the poles ($|\varphi| \sim 60° - 90°$) is only about 0.01 m/s^2, while at latitudes in between $|\varphi| \sim 30° - 60°$ g_n increases almost linearly by 0.01 m/s^2 per 10°.

Three effects, which are obvious but small, are neglected in equation (7):

- A correction due to the height above the earth's radius R_e. In a linear approximation for $h \ll R_e$ we can estimate the contribution as follows:

$$g_0(h) = \frac{\gamma m_e}{(R_e + h)^2} \approx \frac{\gamma m_e}{R_e{}^2}\left(1 - 2\frac{h}{R_e}\right) = g_0 - \frac{\Delta g}{\Delta h} \cdot h\,. \tag{8}$$

  For $R_e = R_{eq}$ we get $\Delta g/\Delta h \sim 3$ µm/s^{2}m which means that if the height h varies up to 2000 m g varies up to 0.006 m/s^2.
- A correction due to mass inhomogeneity up to 2 µm/s^2 [3].
- A time dependent correction due to the tides up to 1 µm/s^2 [4].

As we have demonstrated with the graph $g_n(\varphi)$ in figure 2 the dependency of g on latitude requires an accuracy of 0.01 m/s^2. The total error of $g(\varphi)$ in our measurements is difficult to be estimated or calculated, because several parameters or mathematical dependencies enter in that formula. Therefore, we suggest to compare a measured value for g at a given position on earth (φ, h) with the given theoretical value $g_n(\varphi, h)$. The actual position on earth (φ, h) can be found at national institutes, by a GPS-system or by means of *Google Earth* with sufficient precision.

3. String pendulum to measure $g(\varphi)$

Commonly, relative measurements of g are carried out by precision mechanics devices - the so called gravimeters. They work by the principle of a spring balance. Absolute measurements of g - like we do here - could be done by all kinds of fall experiments. We used a string pendulum, whose geometry and relevant quantities are described in figure 3.

Fig. 3

Table 1

As possible models for this pendulum we discuss in table 1 the mathematical (index m), the physical (index p) and the real pendulum (index r). These models are different with respect to the fact that if the mass of the pendulum is assumed to be concentrated in one point (moment of inertia $J_A = m_{sp}\, l_{AM}{}^2$) or if one has to consider additional forces caused by friction ($\vec{F}_f$) and buoyancy/lifting ($\vec{F}_l$) beside the gravitational force ($\vec{F}_g$). Also in table 1 the final formulas for the determination of g are given [5]. The more we are modelling the real case the more parameters in g have to be considered obviously.

- For the mathematical and physical pendulum we separate between a harmonic and an anharmonic case. If we apply the approximation for small angles (α in rad)

$$mg\sin\alpha \approx mg\alpha \qquad 0 \le \alpha \le 5° \tag{19}$$

  and

$$mg\sin\alpha \le mg\alpha \qquad \alpha \ge 0° \tag{20}$$

  the oscillation period T in the harmonic case is too small by an anharmonicity factor $k > 1$, which depends on the amplitude. To achieve an accuracy of $\Delta g < 0.01$ m/s^2 the initial displacement angle α_0 has to be less than 5°, which corresponds to $k < 1.0005$ according to equation (9) of table 1.

- In case of the physical pendulum the oscillation period T will be mass dependent, because we give up the concept of an ideal centre of mass. The total moment of inertia of the pendulum is the sum of the moment of inertia of the cylindrical string and the spherical mass according to the theorem of Steiner. The centre of mass of the total pendulum is the one respecting the centre of mass of the string and of the sphere.
- In case of the real pendulum we consider here only the harmonic case, in which the frictional Stokes force acting on the moving sphere with velocity v is given by

$$F_{f,S} = const \cdot v_{sp} \tag{21}$$

to avoid too much mathematical approaches. This linear approximation in the frictional term is justified, although typical Reynolds numbers for this string pendulum are much larger than 1, causing a turbulent flow. We proved this justification by a simulation in which we describe the damping of a real pendulum for the Stokes case and for the Newton case

$$F_{f,N} = const \cdot {v_{sp}}^2 , \tag{22}$$

which delivered almost the same damping properties. If we consider the very small force due to buoyancy and due to friction the value for the real pendulum g_r will be slightly larger than that for the physical pendulum g_p since the friction term reduces the restoring force and, therefore, causes a larger oscillation period. In addition, the friction term increases the oscillation period via damping. The damping coefficient has been determined by means of

$$\delta = \ln\left(\frac{\alpha(t=0)}{\alpha(t=nT)}\right)\cdot(nT)^{-1} , \tag{23}$$

where n is the number of oscillations.

After introducing the models of how to describe a pendulum we turn now to measurements and comparison of the results in the different models.

4. Tips and tricks for construction and measurements

In order to determine $g(\varphi)$ with an accuracy of Δg ~ 0.01 m/s^2 one has to pay attention on the following issues:

- To realize the pendulum by a thin cylindrical string (i.e. wire) and a sphere, the wire must be soldered into a hole of the sphere (figure 4a).
- If the wire is clamped between two blocks at point A (see fig. 3) an error in measurements of more than 0.01 m/s^2 will arise, since the wire has a certain stiffness. This stiffness gives rise to the fact, that the effective oscillatory length of the wire is shortened. In consequence, g is measured as too large. This can be avoided if the wire is wind up on a steel pin providing against gliding. The pendulum then has to be hung up in a comb-like holder (figure 4b).
- The gravitational force of the total pendulum mass causes a tension in the wire and, therefore, the static length of the wire can increase on a scale of millimetres. This true length of the string has to be determined (of course with attached spherical mass and after a period of elastic relaxation of the wire).
- During oscillation the mass experiences centrifugal force which causes at maximum a change of wire length of the order of nanometres which can be neglected consequently.
- Before starting to measure the string length, the wire has to be smoothed out. The length can be determined by means of an ordinary, but well calibrated, pocket tape measure with an accuracy of < 0.5 mm (ca. 0.02 % relative error) (figure 4c).

- Changes in temperature of less than 10°C can produce a change in wire length which effects the determination of g of about 0.001 m/s^2. This effect can be either neglected, considered in the measurements or avoided by means of constant room temperature [1].

Fig. 4

In table 2 we present results of two measurements performed in Speyer, Germany. Measurement 1 with small amplitude and practically no damping, measurement 2 with large amplitude and detectable damping.

Table 2

Before starting the actual measurement we have to determine the values ρ_{ls}, r_s, l_s, r_{sp} and m_{sp} by suited tools. During the measurement one has to determine the number of oscillations n, the oscillation periods nT during n oscillations by a light barrier and the horizontal elongation a. In the anharmonicity factor k (see table 1) enters the angle α_0, which we approximate by an averaged angle from the horizontal elongation at the beginning ($a(t = 0)$) and at the end ($a(t = nT)$) of the measurement. In the lower part of table 2 the values of g on the basis of three different pendulum models for the harmonic ($k = 1$) and anharmonic case ($k > 1$) are presented. For the anharmonic real pendulum we used the relation $g_{r,k} = g_{r,1} k^2$ like we did for the other models. As we can recognize from the comparison between the measured value of $g_{r,k}$ and the theoretical value of $g_n(\varphi, h)$ in the last two rows the magnitude of the difference is ca. 0.003 m/s^2 and 0.002 m/s^2 which is below the required accuracy of 0.01 m/s^2.

5. Designing a pendulum (comparison of mathematical and physical pendulum)

The relative error f of g_m with respect to g_p for the same horizontal elongation follows from equation 11 and 15 to be

$$f = \frac{g_m - g_p}{g_p} = \frac{m l_{AS} l_{AM}}{J_A} - 1 . \tag{24}$$

In the case of a physical pendulum with a wire of zero mass $l_{AS} = l_{AM}$ and $m = m_{sp}$, the moment of inertia therefore reads

$$J_A = J_{sp} = m_{sp} l_{AM}{}^2 + \frac{2}{5} m_{sp} r_{sp}{}^2 . \tag{25}$$

The measurement of g then would always produce values of g which are larger than in case of a mathematical pendulum, because

$$f = \left(1 + \frac{2 r_{sp}{}^2}{5 l_{AM}{}^2} \right)^{-1} - 1 < 0 . \tag{26}$$

For a wire with certain mass the relative error f depends on the density ρ_s, length l_s and radius r_s of the wire as well as on the density ρ_{sp} and radius r_{sp} of the sphere (see appendix):

$$f = \left(1 + \frac{3 \rho_s l_s{}^2 r_s{}^2}{8 \rho_{sp} r_{sp}{}^3 (l_s + r_{sp})} \right) \cdot \left(1 + \frac{2 \mathrm{r_{sp}}{}^2}{5 (l_s + r_{sp})^2} + \frac{\rho_s l_s{}^3 r_s{}^2}{4 \rho_{sp} r_{sp}{}^2 (l_s + r_{sp})^2} \right)^{-1} - 1 . \tag{27}$$

---

[1] The time delay of Richer's pendulum clock could also be partially caused by the higher temperature in Cayenne. We notice that the compensation pendulum (Graham 1721) and the steel alloy Invar (Guillaume 1896), which has a very low coefficient of thermal expansion, were not invented at that time. For example, a temperature difference of $\Delta t = 20$°C, a pendulum length $l_{AM} = 1$ m, a coefficient of thermal expansion of $\alpha_s = 1{,}5 \cdot 10^{-5}$/K and $g_{Pa} = 9.811$ m/s^2 gives for a mathematical pendulum a shift of ca. 26 s/day.

If we use the values of our pendulum here (see table 2) and if we consider the sphere radius as an independent variable then f tends to zero for a sphere of radius 3.7 cm (figure 5). But such a sphere made out of steel is weighing 1.67 kg and is producing a wire tension of about 520 N/mm^2. This tension exceeds the tensile strength of ca. 400 N/mm^2 of the used constantan wire. So the question is which parameters have to be varied in order to lower the value for the sphere radius r_K and, therefore, the mass of the sphere.

Fig. 5

We will now briefly discuss different possible approaches to solve this problem.

- A smaller wire radius r_s causes a lower value for tension fracture, therefore, this is not a solution.
- A shorter wire length l_s causes an increase of the relative error of the length which should be avoided.
- Since we need a magnetic material for the sphere (see next section) materials of larger density like lead cannot be used.

To set up such a string pendulum for which $f \sim 0$ requires a wire material with a very large tensile strength as for example a special type of steel alloy (Remanium©).[2] In conclusion, it is not a simple task to set up a string pendulum for precise *g*-measurement.

6. World Pendulum as remote lab

With a Remotely Controlled Laboratory (RCL) a user at a location A (with client computer) can perform a real experiment located at B via Internet (figure 6). To control this experiment and for measurements an interface connects the experiment with a web server. A web cam allows the client user to watch in real time what is going on at the experiment. Details about our remote labs can be read in ref. [6] or obtained by visiting the website of the project [7].

Fig. 6

In order to determine $g(\varphi)$ the user must be able to measure time intervals Δt and numbers of oscillations n during these intervals. Furthermore, the remote user must have access to the experiment in that way, that he or she can initially elongate the sphere and start the oscillations of the pendulum. To elongate the sphere at the beginning of the experiment, a movable coil has to be driven close to the sphere and by remotely turning on a switch of a power supply the current in the coil lets act it as an electromagnet. By this technique the position of the sphere (initial elongation) can be varied in a certain range. The measurement of time intervals is enabled by a light barrier connected to an electronic counter/timer unit. Via web cam the user can observe the experiment and the lab control frame of the web site displays the oscillation period as well as the numbers of oscillations.

7. Teaching environment

Global experimenting

We are planning to set up a cluster of several world pendulums with respect to the degree of latitude; to begin with this network we already have five cooperating institutes distributed at different places at the northern hemisphere (see Fig. 2). According to our remote lab technology a client user from somewhere on earth can then control these pendulums to perform measurements of $g(\varphi)$. The Internet allows the cooperative data collection of a global phenomenon: each user can communicate his or her values of $g(\varphi)$ in a table on the world pendulum web site. To compare experimental and theoretical values the measured values of $g(\varphi)$ can be put into a diagram according to Fig. 2, which will grow continuously.

Teaching level

[2] This steel alloy is used as wire material for dental purposes (wire mounting of braces). It has a tensile strength of 1900 N/mm² (manufacturer: Dentaurum, Germany, http://www.dentaurum.de/eng/).

At school level we offer a topic for mini-research: to perform accurate measurements, to discuss impact of errors in measurements, to understand approximations. This topic may fit in several positions of the curriculum: in mechanics generally, in oscillations, in measuring forces, in rotational motion and frames of reference, in history of physics. Finally, modern kind of programming, interfacing, measuring devices will be used.
At university level all three kinds of pendulums (see table 1 – mathematical, physical and real pendulum) will be presented mathematically with all necessary approximations. The contribution of all factors when determining $g(\varphi)$ experimentally, as discussed above, may give the opportunity to treat that in exercises, for example. It is expected that the user at this level should understand the programming, interfacing, data acquisition and measuring devices in detail.

New ways of teaching / learning
This experiment and its physical topic can be worked out as a project, in groups and in self placed manner. One may put a specific emphasis on the physical, mathematical, technical and/or Internet aspect. In general, we are teaching in class locally in space and time; whereas here the global aspect is advantageous: from everywhere on earth at any time the network of pendulums can be accessed and controlled. The discussion of measured values $g(\varphi)$ may happen in different languages beyond all groups of learners.

If the reader is interested in taking part of the World Pendulum project we suggest to contact us.

8. Appendix

In order to get equation 27 we make use of the equations 24, 12 and 13:

$$f = \frac{m l_{AM} l_{AS}}{J_A} - 1$$

$$= \left(m_{sp} l_{AM}{}^2 + \frac{m_s l_s l_{AM}}{2} \right) \cdot \left(\mathrm{m_{sp} l_{sp}}^2 + \frac{2}{5} \mathrm{m_{sp} r_{sp}}^2 + \frac{1}{3} \mathrm{m_s} l_s{}^2 \right)^{-1} - 1$$

$$= \left(1 + \frac{m_s l_s}{2 m_{sp} l_{AM}} \right) \cdot \left(1 + \frac{2 \mathrm{r_{sp}}^2}{5 \mathrm{l_{AM}}^2} + \frac{1}{3} \frac{m_s l_s{}^2}{m_{sp} l_{AM}{}^2} \right)^{-1} - 1 \qquad \text{A.1}$$

Inserting the ratio m_s/m_{sp} of the masses of the string and the sphere

$$\frac{m_s}{m_{sp}} = \frac{\rho_s \pi r_s{}^2 l_s}{\rho_{sp} \frac{4}{3} \pi r_{sp}{}^3} = \frac{3 \rho_s l_s r_s{}^2}{4 \rho_{sp} r_{sp}{}^3} \qquad \text{A.2}$$

and the expression for the length l_{AM}

$$l_{AM} = l_s + r_{sp} \qquad \text{A.3}$$

in equation A.1 we arrive at the final formula for the relative error f:

$$f = \left(1 + \frac{3 \rho_s l_s{}^2 r_s{}^2}{8 \rho_{sp} r_{sp}{}^3 (l_s + r_{sp})} \right) \cdot \left(1 + \frac{2}{5} \frac{\mathrm{r_{sp}}^2}{(l_s + r_{sp})^2} + \frac{\rho_s l_s{}^3 r_s{}^2}{4 \rho_{sp} r_{sp}{}^2 (l_s + r_{sp})^2} \right)^{-1} - 1 \qquad \text{A.4}$$

9. References

[1] Kertz W, Glaßmeier K-H and Kertz R 2002 *Biographisches Lexikon zur Geschichte der Geophysik* (Braunschweig: Braunschweigische Wissenschaftliche Gesellschaft)

[2] White H L 1986 *World geodetic system 1984 - Earth gravitational model* (Springfield: National technical information service)

[3] Klingelé E and Hollenstein C 2005 *Gravimetrie* (online resource: http://www.earthquake.ethz.ch/education/feldkurs/grav_skript)

[4] Graf A 1967 *Gravimetrische Instrumente und Messmethoden. Handbuch der Vermessungskunde* (Stuttgart: Metzlersche Verlagsbuchhandlung)

[5] Walcher W 1985 *Praktikum der Physik* (Stuttgart: Teubner)

[6] Gröber S, Vetter M, Eckert B and Jodl H-J 2007 Experimenting from a distance - Remotely Controlled Laboratory (RCL) appears in *Eur. J. Phys.*

[7] Homepage of the project “Remotely Controlled Laboratory”: http://rcl.physik.uni-kl.de

Tables

Table 1. Models for pendulums to determine the earth's effective gravitational acceleration g.

Pendulum model	**Determination of g**	
Mathematical pendulum $J_A = m_{sp} l_{AM}^2$ $F_l = F_f = 0$	$k = 1 + \left(\frac{1}{2}\right)^2 \sin^2 \frac{\alpha_0}{2} + \left(\frac{1 \cdot 3}{2 \cdot 4}\right)^2 \sin^4 \frac{\alpha_0}{2} + \left(\frac{1 \cdot 3 \cdot 5}{2 \cdot 4 \cdot 6}\right)^2 \sin^6 \frac{\alpha_0}{2} + \ldots$	(9)
	$T = 2\pi \sqrt{\frac{l_{AM}}{g_{m,k}}} \cdot k \qquad g_{m,k} = \frac{4\pi^2 l_{AM}}{T^2} \cdot k^2$	(10,11)
Physical pendulum $J_A \neq m_{sp} l_{AM}^2$ $F_l = F_f = 0$	$J_A = \mathrm{m_{sp} l_{sp}}^2 + \frac{2}{5} \mathrm{m_{sp} r_{sp}}^2 + \frac{\mathrm{m_s} l_s^2}{3} \qquad l_{AS} = \frac{m_{sp} l_{AM} + \frac{m_s l_s}{2}}{m_{sp} + m_s}$	(12,13)
	$T = 2\pi \sqrt{\frac{J_A}{m g_{p,k} l_{AS}}} \cdot k \qquad g_{p,k} = \frac{4\pi^2 J_A}{T^2 m l_{AS}} \cdot k^2$	(14,15)
Real pendulum $J_A \neq m_{sp} l_{AM}^2$ $F_l \neq 0$, $F_f \neq 0$	$\alpha(t) = \alpha_0 e^{-\delta t} \cos(\frac{2\pi}{T} t) \qquad \delta = \frac{c_s l_{AS}^2}{2 J_A}$	(15,16)
	$(2\pi / T)^2 = \frac{(m - \rho_a V) g_{r,1} l_{AS}}{J_A} - \delta^2 \qquad g_{r,1} = \frac{(4\pi^2 / T^2 + \delta^2) J_A}{(m - \rho_a V) l_{AS}}$	(17,18)

Table 2. Results of measurements of effective gravitational acceleration *g* at location Speyer, Germany (see discussion in text).

parameter	**Experiment 1**	**Experiment 2**
φ in degrees	49.3176	
h in m	~ 100	
ρ_{ls} in g/m	0.0002825	
r_s in mm	0.1	
r_{sp} in cm	2.0	
m_{sp} in g	260.54	
l_s in m	2.705	
n	20	100
nT in s	66.2119	331.4539
$a(t = 0)$ in cm	3.0	38.3
$a(t = nT)$ in cm	3.0	29.0
k	1.0000076	1.000944
δ in 1/s	~ 0	0.00084
T in s	3.3106	3.3145
$g_{m,1}$ in m/s^2	9.816	9.792
$g_{m,k}$ in m/s^2	9.816	9.811
$g_{p,1}$ in m/s^2	9.811	9.788
$g_{p,k}$ in m/s^2	9.811	9.806
$g_{r,1}$ in m/s^2	9.813	9.789
$g_{r,k}$ in m/s^2	9.813	9.808
$g_n(\varphi,h)$ in m/s^2	9.810	

Figures

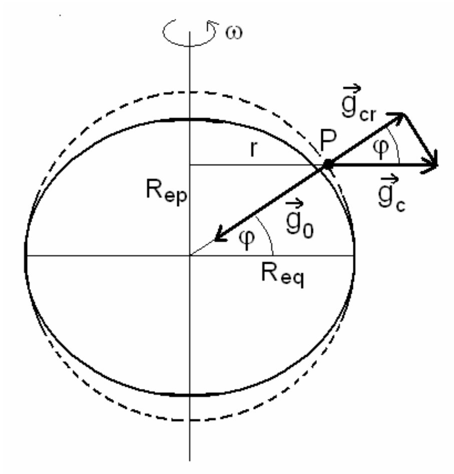

Figure 1. Dynamical contribution on effective acceleration g_{eff}.

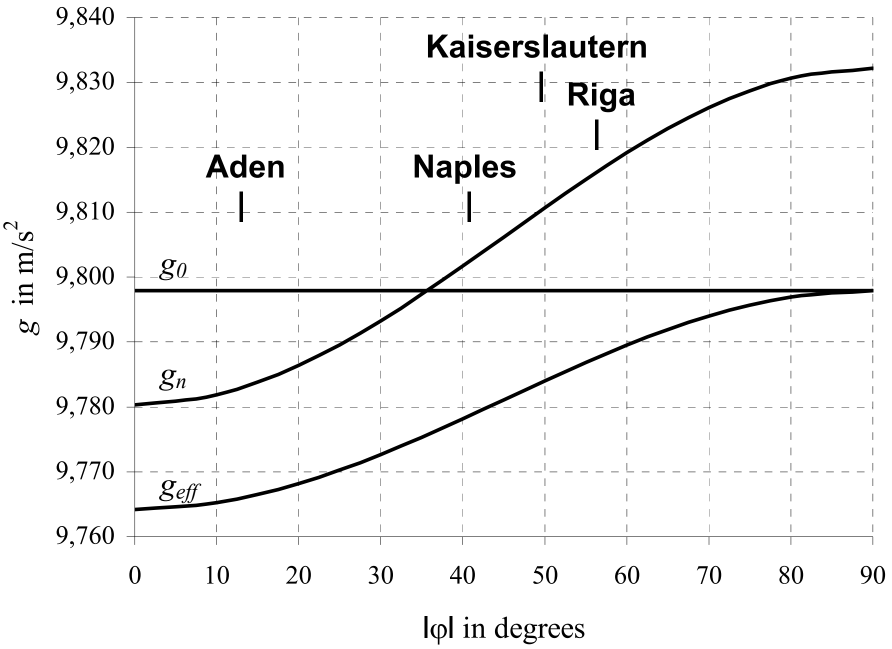

Figure 2. Graphical representation of the results of models for the earth's gravitational acceleration: earth at rest (g_0), rotating spherical homogeneous earth (g_{eff}) and ellipsoidal rotating earth (g_n). The geographical latitude of the cooperating institutes of the World Pendulum project are inserted.

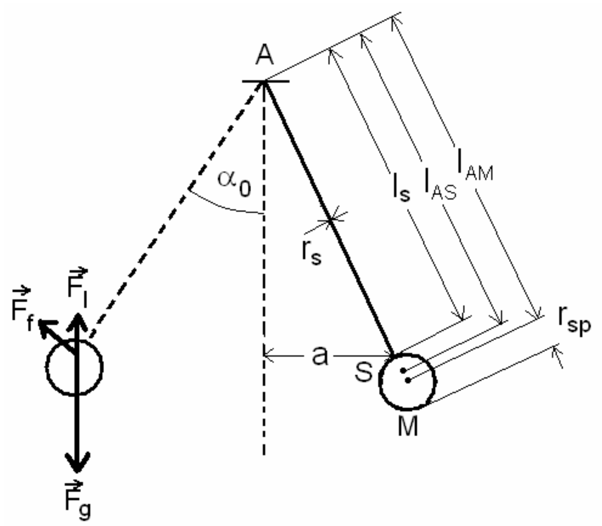

- string: length l_s, radius r_s, density ρ_s, density per length unit ρ_{ls}, mass m_s, moment of inertia with respect to A J_s.
- sphere: radius r_{sp}, mass m_{sp}, moment of inertia with respect to A J_{sp}, velocity v_{sp}.
- forces: gravitation $\vec{F}_g$, total friction $\vec{F}_f$, buoyancy/lifting $\vec{F}_l$.
- additional parameters: initial elongation angle α_0, horizontal distance to vertical axis a, rotation centre of pendulum in A, centre of mass of pendulum S, centre of sphere M, distance AS = l_{AS}, distance AM = l_{AM}, number of oscillations n, oscillation period T, density of air ρ_a volume of pendulum V, total mass of pendulum m, moment of inertia of total pendulum with respect to point A J_A.

Figure 3. Parameters in our string pendulum.

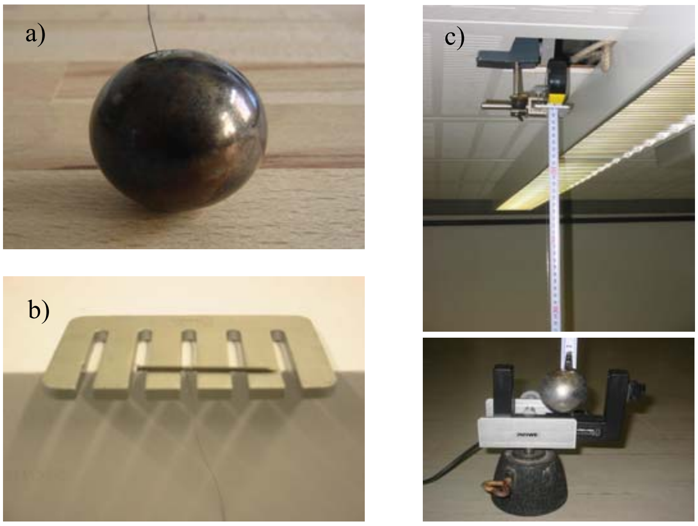

Figure 4. Sphere of the pendulum with soldered wire (a), suspension of the pendulum by means of a pin mounted on a comb (b), determination of wire length by a pocket tape measure (c).

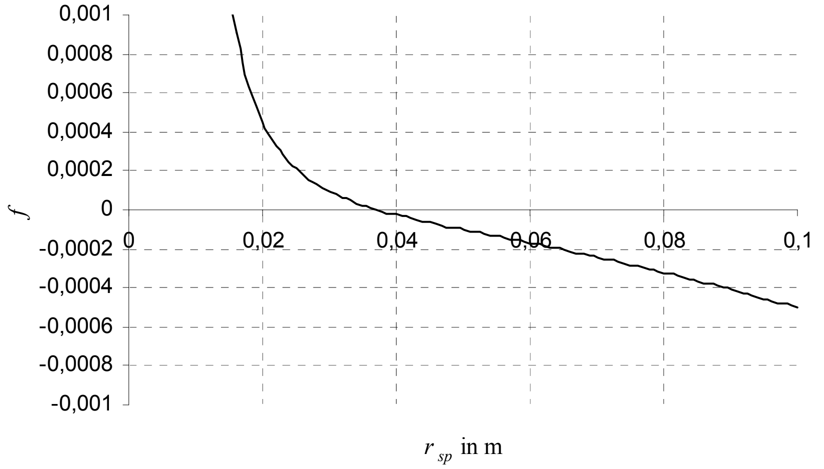

Figure 5. Graph of relative error f of g_m with respect to g_p for ρ_{sp} = 7,87 g/cm^3 (steel), ρ_s = 8,8 g/cm^3 (constantan), r_s = 0,1 mm and l_s = 2,705 m.

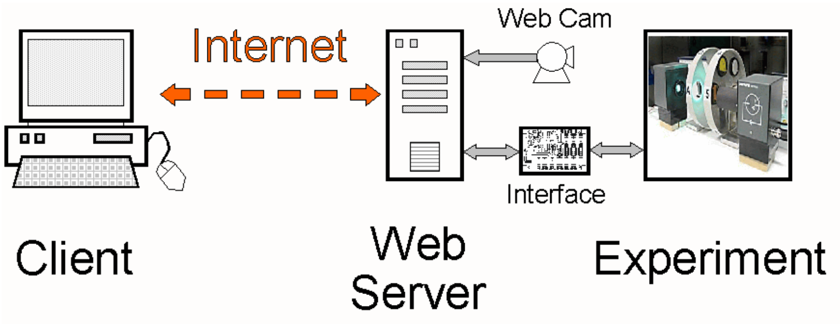

Figure 6. Simplified schematic sketch of a remote lab.